American Mineralogist, Volume 70, pages 332–343, 1985

High-resolution ^{29}Si NMR study of silicate and aluminosilicate glasses: the effect of network-modifying cations

JAMES B. MURDOCH,[1] JONATHAN F. STEBBINS

Earth Sciences Division
Lawrence Berkeley Laboratory, Berkeley, California 94720

AND IAN S. E. CARMICHAEL[2]

Department of Geology and Geophysics
University of California, Berkeley, California 94720

Abstract

The effect of network-modifying alkali and alkaline-earth cations on the degree of polymerization in silicate glasses is investigated using ^{29}Si magic-angle spining NMR. The NMR linewidth is found to increase (reflecting a broader range of silicate environments) as the polarizing power of the cation increases. A similar effect occurs in three-dimensional framework aluminosilicate glasses: smaller, more highly charged cations create greater variety in the distribution of silicate and aluminate tetrahedra. Linewidths as a function of the silicon-to-aluminum ratio suggest, however, that Loewenstein's aluminum avoidance principle is largely obeyed. Spectra of three natural silicic glasses are analyzed in terms of the Si/Al ratio and the concentration of paramagnetic species.

Introduction

The structure of silicate glasses is of interest not only with regard to their commercial applications but also in that they are frozen approximations of silicate melts, for which a detailed knowledge of silicate speciation is needed to better understand magmatic processes. As such, silicate glasses have been studied using a variety of techniques, notably Si$K\beta$ X-ray absorption (de Jong et al., 1981), X-ray radial distribution functions (RDF's) (Konnert and Karle, 1973; Taylor and Brown, 1971a, 1979b), laser Raman spectroscopy (e.g., Brawer and White, 1975; Mysen et al., 1982; McMillan, 1984a; Matson et al., 1983), and nuclear magnetic resonance (NMR) spectroscopy (Holzman et al., 1956; Mosel et al., 1974; Harris and Bray, 1980; de Jong and Schramm, 1981; Lippmaa et al., 1982; Kirkpatrick et al., 1982; de Jong et al., 1983).

In nuclear magnetic resonance spectroscopy, a nucleus with non-zero spin is used as a sensitive probe of its local electronic environment. The most useful parameter obtained is the chemical shift (or shielding) which characterizes the degree to which nearby electrons shield the probe nucleus from a large external magnetic field. Nuclei in different bonding sites or environments are shielded differently and hence absorb energy at different frequencies.

In a polycrystalline solid, however, spectral features are broadened by the orientational anisotropy of chemical shielding and by interactions between nuclei. By rapidly spinning a powdered sample at the magic angle, 54.7°, relative to the external magnetic field, the broadened lineshape breaks up into a center peak located at the isotropic chemical shift plus a series of spinning sidebands spaced at the rotational frequency, typically 1-4 kHz (Andrew, 1971; Maricq and Waugh, 1979). For crystalline samples, sideband intensities can be analyzed to obtain the principal values of the chemical shielding tensor (Maricq and Waugh, 1979; Herzfeld and Berger, 1980; Smith et al., 1983), but are often made negligible by spinning rapidly compared to the static linewidth expressed in Hz. One can obtain wellresolved spectra of isotropic chemical shifts, similar to NMR spectra commonly obtained from liquids.

At least four magnetically active nuclei have been used in studying silicate minerals with magic-angle spinning (MAS) NMR: silicon-29, aluminum-27, sodium-23, and oxygen-17. Of these, ^{29}Si has the advantage that its spectra are intrinsically better resolved. Unlike ^{29}Si, the other three nuclei with spin $I > 1/2$ have a quadrupolar charge distribution and hence are affected by local electric field gradients (Abragam, 1961, Chap. 6). In a polycrystalline sample, this nuclear quadrupole interaction gives rise to a broadening of the center MAS peak that cannot be removed by magic-angle spining. The broadening can be so severe for nuclei (such as ^{27}Al) in distorted sites that no measurable NMR signal is obtained (de Jong et al., 1983). In contrast, the width of a ^{29}Si MAS NMR peak for a non-paramagnetic glassy sample reflects merely the range of isotropic shifts therein, and the spectrum can provide a quantitative measure of relative site populations if the delay between succesive rf pulses is long enough to allow all relevant nuclei to fully equilibrate.

[1] Present address: Technicare Corporation, P.O. Box 5130, Cleveland, Ohio 44101.

[2] Reprint requests should be addressed to I.S.E. Carmichael.

0003–004X/85/0304–0332$02.00

A second virtue of ^{29}Si NMR spectroscopy is that isotropic chemical shifts vary systematically as a function of silicate structure. Lippmaa et al. (1980) first observed distinct ^{29}Si chemical shift ranges for different types of silicate structural units in crystalline materials, specifically, that a silicon nucleus is deshielded (and its chemical shift δ measured relative to a tetramethylsilane standard becomes less negative) as the number of attached Si–O–Si bridging oxygens decreases. Later measurements (Smith et al., 1983; Grimmer et al., 1983b, 1983c; Mägi et al., 1984) on a larger and more varied collection of silicates indicated an appreciable overlap of the isotropic chemical shift ranges associated with different Q^n species, where Q^n is short for an $Si(O\text{–}Si)_n\ (O\text{–}M)_{4-n}$ unit (Engelhardt et al., 1975). (Here n is the number of bridging oxygens; 4 − n is the number of non-bridging oxygens, which serve to coordinate a network-modifying cation M.)

The silicon chemical shift is also affected by the number of adjacent aluminate tetrahedra. In tectosilicates (Q^4 units), for example, silicon nuclei are deshielded and δ becomes less negative as the number of neighboring aluminum atoms increases from zero to four (changing typically by ~5 ppm per Si–O–Al linkage). Table 1 lists the experimentally determined chemical shift ranges associated with each of these species, as compiled by Thomas et al. (1983b). The reasonably good separation in these shift ranges has greatly facilitated the study of silicon-aluminum ordering in zeolites (Lippmaa et al., 1981., Klinowski et al., 1982; Thomas et al., 1983b).

Additionally, isotropic silicon chemical shifts have been correlated with a number of more general crystalline structural parameters. The value of δ becomes more negative with a decrease in the average Si–O bond length (Higgins and Woessner, 1982), an increase in the total cation–oxygen bond strengths for all the oxygens in the silicate tetrahedron (Smith et al., 1983), and for tectosilicates, an increase in the average Si–O–Si bond angle (Smith and Balckwell, 1983; Thomas et al., 1983a); (Ramdas and Klinowski, 1984). A similar dependence on the Si–O–Si bond angle has been found for the ^{29}Si chemical shift in a series of sorosilicates with distinct $Si_2O_7^{6-}$ anions (Grimmer et al., 1983b).

In this paper, isotropic ^{29}Si chemical shifts from MAS spectra will be used to investigate the range of silicon environments in glasses, specifically the degree of polymerization in disilicate and metasilicate glasses, the variation in Si–O–Si bond angles in silica glass, and the distribution of silicate and aluminate tetrahedra in three-dimensional framework aluminosilicate glasses.

Table 1. Isotropic ^{29}Si chemical shift ranges (relative to TMS) for Q^4 units in crystalline aluminosilicates*

Silicate species	Range of δ values (ppm)
$Si(\text{-}OAl)_4$	-80 to -90.5
$Si(\text{-}OAl)_3(\text{-}OSi)_1$	-88 to -97
$Si(\text{-}OAl)_2(\text{-}OSi)_2$	-93 to -102
$Si(\text{-}OAl)_1(\text{-}OSi)_3$	-97.5 to -107
$Si(\text{-}OSi)_4$	-101.5 to -116.5

*from Thomas et al. (1983b)

Experimental

Sample preparation

Glasses were prepared from reagent grade alkali and alkaline earth carbonates and dehydrated silicic acid, and were fused and ground several times to insure homogeneity. Wet chemical and electron microprobe analyses indicate that the desired compositions were obtained with the following exceptions, (which we consider to be inconsequential to the results reported here): the $BaSi_2O_5$ sample contains approximately 1 wt.% SrO, and the $MgSiO_3$ glass contains approximately 0.5 wt.% Al_2O_3.

To prevent crystallization, $NaAlSiO_4$, $CaSiO_3$, and $MgSiO_3$ glasses were quenched in water; liquid nitrogen was used for lithium and sodium disilicate glasses to prevent crystallization and possible unmixing. Strontium disilicate glass was quenched by pouring the melt onto a graphite slab. The thick pieces that resulted in this composition were opalescent due to metastable phase separation during cooling. Smaller, more rapidly quenched pieces were clear, and these were selected for NMR use. Other glasses were quenched in air. The hygroscopic alkali silicate glasses were crushed for NMR work in an N_2-filled glove box and were subsequently handled for only brief periods of time in air. All samples were stored in vacuum dessicators.

Samples of the alkali and alkaline earth disilicate glasses were crystallized at 700°C for roughly 24 hours. $MgSiO_3$ glass was crystallized at about 1400°C for several days. The crystalline material was therefore originally protoenstatite that transformed to clino- or possibly a mixture of clino- and ortho-enstatite on quench.

Spectroscopy

All spectra were recorded on a home-built Fourier transform NMR spectrometer operating at 8.5 Telsa. Powdered samples were packed in alumina rotors and spun at roughly 3 kHz in a magic-angle spinning probe from Doty Scientific. (The angle was adjusted by maximizing ^{127}I rotational echoes from a sample of NaI). From 190 to 1040 free induction decays were averaged together for each glass; the rf pulse flip angle was approximately 32° and the delay between pulses was 120 sec unless noted otherwise. Silicon chemical shifts were measured relative to an external sample of tetramethylsilane (TMS) and are reported to the nearest 0.5 ppm.

Results and discussion

Alkali and alkaline earth silicate glasses

We first will consider the effects of alkali and alkaline earth cations on the network structure of disilicate and metasilicate glasses. To interpret their MAS NMR spectra, we turn to the ^{29}Si chemical shifts of related crystalline compounds, listed in Table 2. In this restricted but relevant assemblage of silicates, chemical shift ranges are fairly well separated for different Q^n species, changing by roughly ten ppm with the conversion of each non-bridging oxygen (NBO) to a bridging one. Caution is of course required in

Table 2. Isotropic ^{29}Si chemical shifts for crystalline alkali and alkaline earth silicates and SiO_2 polymorphs

	Silicate*	δ (ppm from TMS)	Reference**	Polymorph
Q^0				
	Mg_2SiO_4	-62	1	
	$CaMgSiO_4$	-66	2	
Q^1				
	$Li_6Si_2O_7$	-72.4	3	
	$Na_6Si_2O_7$	-68.4	3	
	$Ca_3Si_2O_7$	-74.5,-76.0	3	rankinite
	$Ca_2MgSi_2O_7$	-73	2	
Q^2				
	$MgSiO_3$	-81,-83.5	1	clinoenstatite†
	$CaMgSi_2O_6$	-84	2	
	$CaSiO_3$	-88.5	1	wollastonite
	$SrSiO_3$	-85	2	
	$BaSiO_3$	-80	2	
Q^3				
	$Li_2Si_2O_5$	-92.5	1	
	$Na_2Si_2O_5$	-94.5	1	α-form†
	$K_2Si_2O_5$	-91.5,-93,-94.5	1	
	$BaSi_2O_5$	-93.5	1	
Q^4				
	SiO_2	-107.1	4	quartz
	SiO_2	-108.5	4	cristobalite
	SiO_2	-108.1,-113.9	4	coesite

*all synthetic except $CaSiO_3$ (from Willsboro, NY) and the silica polymorphs

**1 = this work; 2 = Smith et al., 1983; 3 = Grimmer et al., 1983b; 4 = Smith and Blackwell, 1983

†assumed polymorph based on devitrification conditions

assigning specific Q^n units on the basis of ^{29}Si chemical shifts since the value of δ can change by as much as 25 ppm depending on Si–O–Si bond angles (Grimmer et al., 1983b). Nonetheless, if it is assumed that no radical difference in bond angle distribution exists between glass and crystal, the variation of silicate polymerization in glasses as a function of network-modifying cations can be estimated from the crystalline chemical shift differences in Table 2.

There is a much broader range of silicate environments in a glass than in the corresponding crystalline material, as reflected in the MAS NMR spectra of enstatite ($MgSiO_3$, a pyroxene with single chains of Q^2 tetrahedra) and enstatite glass in Figure 1. The width of the glass peak is due in part to variations in Si–O–Si bond angles and Si–O bond lengths, these being a natural consequence of the lack of long-range order. In addition, there is the possibility of variation in the number of non-bridging oxygens per silicate tetrahedron. Indeed, the $MgSiO_3$ glass peak encompasses the entire chemcial shift range from Q^0 to Q^4 units.

For disilicate glasses like $Na_2Si_2O_5$, the following equilibrium has been proposed to describe the nature of silicate polymerization (Virgo et al., 1980):

$$Si_2O_5^{2-} \rightleftharpoons SiO_3^{2-} + SiO_2, \quad (1)$$

where $Si_2O_5^{2-}$, SiO_3^{2-}, and SiO_2 refer to structural units with sheet-like, chain-like, and three-dimensional framework environments respectively.

More generally one can write

$$2Q^3 \rightleftharpoons Q^2 + Q^4, \quad (2)$$

where only the relative number of bridging and non-bridging oxygens rather than an extended silicate geometry is specified (Matson et al., 1983). For metasilicate glasses like $MgSiO_3$, equilibria such as

$$2Q^2 \rightleftharpoons Q^1 + Q^3 \quad (3)$$

or

$$2Q^2 \rightleftharpoons Q^0 + Q^4 \quad (4)$$

can be envisaged.

Different network-modifying cations are expected to shift these glass equilibria to the left or to the right. To the left implies the same type of silicate polymerization as they found in the corresponding crystal, with a more-or-less evenly spaced distribution of cations. To the right implies a bunching of cations near those silicate units with extra non-bridging oxygens and a paucity of cations near those with fewer NBO's.

The ^{29}Si MAS NMR spectra of potassium, sodium, and lithium disilicate glasses are displayed in Figure 2, those of barium and strontium disilicate glass in Figure 3, and those of the metasilicate glasses $CaSiO_3$, $CaMgSi_2O_6$, and $MgSiO_3$ in Figure 4. Each center peak is flanked by a pair or two of spinning sidebands, but the intensities of these will not be analyzed here. The $Li_2Si_2O_5$ glass spectrum is much narrower than the one reported by de Jong and Schramm (1981) and more nearly resembles their partially devitrified $Li_2Si_2O_5$ spectra. We have no indication, however, that our glass has devitrified.

Three observations regarding the center peaks in Figures 2–4 are immediately apparent. First, most of the peaks are

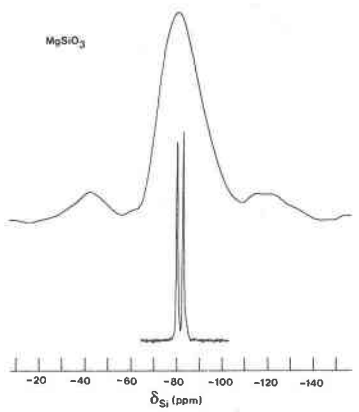

Fig. 1. ^{29}Si MAS NMR spectra of glassy and crystalline $MgSiO_3$. The full widths at half maximum are 22.7 and 0.8 ppm respectively. The two peaks in the lower spectrum correspond to two crystallographically distinct positions for silicon in clinoenstatite (Ohashi and Finger, 1976).

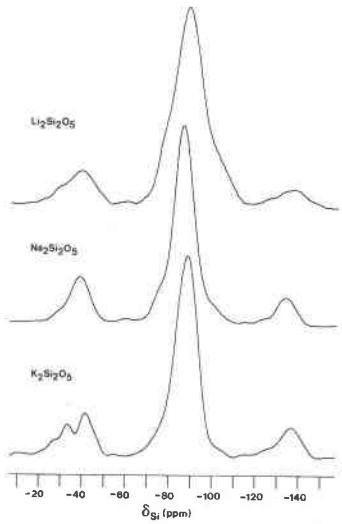

Fig. 2. ^{29}Si MAS NMR spectra of alkali disilicate glasses. The dip in the left spinning sideband of $K_2Si_2O_5$ is an artifact. Peak heights are normalized in this and subsequent figures.

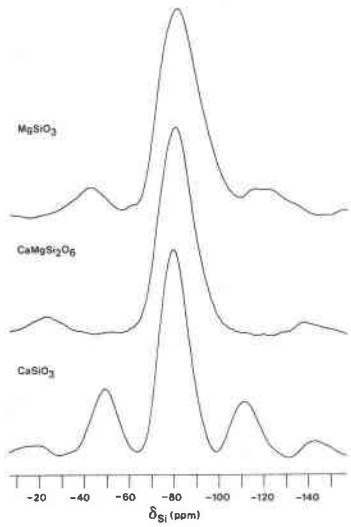

Fig. 4. ^{29}Si MAS NMR spectra of alkaline earth metasilicate glasses.

featureless, with no distinct "bump" for each Q^n species. This lack of structure results from the fact noted earlier that the silicon chemical shift is sensitive to variations in bond lengths and angles as well as the degree of polymerization. Only the spectra of sodium and lithium disilicate glasses have noticeable shoulders. (Indeed, the only glass for which we have seen distinct Q^n species is $Na_2Si_2O_9$, which contains an average of 3.5 bridging oxygens per Si. Its ^{29}Si MAS spectrum contains two central peaks of roughly equal intensity at -92.5 and -104.5 ppm, the former with a sideband intensity pattern much like that of $Na_2Si_2O_5$ glass, the latter without sidebands. These peaks reflect the presence of well-defined Q^3 and Q^4 units. The sample, which is rapidly quenched and optically clear, is currently being examined for sub-microscopic phase separation).

Second, in each case the position of the peak maximum indicates that the dominant silicate species present in the glass is the one found in the corresponding crystalline material, namely Q^3 units in disilicates and Q^2 units in metasilicates. This finding is consistent with previous MAS NMR results (Kirkpatrick et al., 1982), with Raman work (Brawer and White, 1975; Mysen et al., 1983; Matson et al., 1983), with an RDF measurement on $Na_2Si_2O_5$ glass (Imaoka et al., 1983), and in general with the results of de Jong et al. (1981) from Si$K\beta$ spectroscopy (although we see no evidence for bimodal Q^n distributions).

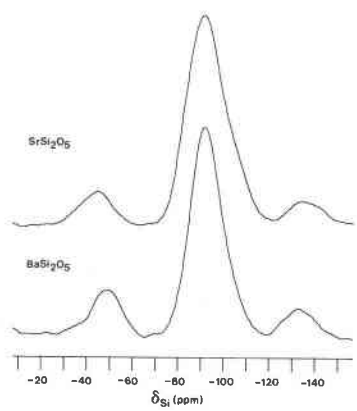

Fig. 3. ^{29}Si MAS NMR spectra of alkaline earth disilicate glasses.

Third, in each of Figures 2–4, the chemical shift range encompassed by the glass peak increases as the size of the cation decreases. These trends suggest the greater the polarizing power of a network-modifying cation, the more it will disrupt a silicate structure, shifting the equilibria discussed earlier to the right, localizing the negative charge associated with NBO's, and creating a broader range of silicate species. Again, the result agrees with Raman findings (Brawer and White, 1975; Mysen et al., 1982; Matson et al., 1983; McMillan, 1984b). This interpretation of silicate liquid speciation is also consistent with, and was ultimately inspired by, work on the effect of cation substitution on the chemical activity of SiO_2 in binary melts (e.g., Charles, 1967).

A complementary description, in accord with CNDO/2 molecular orbital calculations (de Jong et al., 1981), is that smaller cations prefer to cluster together: as an example, the creation of silicate units with multiple O-M linkages tends to be energetically favorable for M = Li but not so for M = K.

Table 3 lists the integrated linewidths for each of the MAS glass spectra. Calculated as the area under a center peak divided by its height. (This measure is more sensitive than the full width at half maximum to variations in peak shape, particularly to the occurrence of small shoulders). These linewidths are plotted in Figure 5 as a function of the polarizing power (or ionic potential) of the network-

Table 3. Isotropic peak positions and linewidths in the ^{29}Si MAS NMR spectra of disilicate and metasilicate glasses

Glass	Peak position (ppm from TMS)	Integrated linewidth (ppm)
$K_2Si_2O_5$	-90.5	13.2
$Na_2Si_2O_5$	-88.5	13.0
$Li_2Si_2O_5$	-90.5	18.7
$BaSi_2O_5$	-92.5	17.6
$SrSi_2O_5$	-92.5	21.3
$CaSiO_3$	-81.5	15.3
$CaMgSi_2O_6$	-82.0	18.0
$MgSiO_3$	-81.5	22.0

modifying cation, simply the ionic charge divided by an appropriate ionic radius in nm. [A number of other cation properties—ionization potentials, field strengths, molecular orbital mixing coefficients (de Jong et al., 1981), etc.—could be used as well with the same qualitative result.] For both disilicates and metasilicates, the trend towards a wider Q^n distribution in glasses with smaller, more highly charged cations is apparent.

It is curious, however, that the two lines in Figure 5 are displaced, or to be specific, that the linewidth of $CaSiO_3$ glass is noticeably less than that of $SrSi_2O_5$ glass. This difference in width can be partially attributed to the fact that the separation between Q^4 and Q^3 chemical shift ranges in Table 2 is larger than that between Q^3 and Q^2, Q^2 and Q^1, or Q^1 and Q^0. Because of the higher overall level of polymerization, there are in general more Q^4 tetrahedra in disilicate glasses than in metasilicate glasses, and the higher concentration of these Q^4 silicons gives rise to extra broadening of the disilicate MAS peaks. (The nonlinearity in the relationship between chemical shift and degree of polymerization is also the likely cause of the peak asymmetries in Figures 3 and 4.) The difference in disilicate and metasilicate glass linewidths may in addition reflect a larger equilibrium constant for reaction (2) than for reations (3) and (4).

The pronounced shoulders in the lithium disilicate glass spectrum, implying more clearly defined Q^n units than in the other glass samples, are probably related to its propensity to separate into reigons of higher and lower lithium content (Tomozawa, 1972). A deconvolution of the lineshape into three Gaussians yielded peaks at −78.5, −90.5, and −105 ppm with relative intensities of roughly 8:81:11. These we assign to Q^2, Q^3, and Q^4 silicate units respectively. To determine whether the silicon nuclei giving rise to these peaks have different spin-lattice (T_1) relaxation times, free induction decays were accumulated with rf pulse spacings of 15, 120, and 600 seconds. A difference in relaxation times would be a possible indication of distinct lithium-rich and lithium-poor regions, but no appreciable change in lineshape as a function of pulse cycle time was observed.

The $Na_2Si_2O_5$ glass spectrum was also deconvoluted into three Gaussian peaks at −77, −88.5 and −99.5 ppm (Q^2, Q^3, and Q^4 units) with relative intensities of 8:84:8. Furthermore, the signal-to-noise ratio of the full spectrum is high enough that we believe the small bump at −62.5 ppm is probably a real feature, one we ascribe to isolated SiO_4^{4-} tetrahedra (Q^0 units). Its intensity is 0.4% of the main peak and may be present in the $Li_2Si_2O_5$ spectrum as well.

In most of the spectra presented here, the maximum of the glass peak is within a few ppm of the corresponding crystalline peak(s). One exception is $CaSiO_3$, for which the glass maximum appears at −81.5 ppm, whereas the spectrum of crystalline $CaSiO_3$ features one fairly broad peak at −88.5 ppm. In comparison, peak maxima for crystalline and glassy samples of both $CaMgSi_2O_6$ and $MgSiO_3$ lie between −81 and −84 ppm. This difference suggests that crystalline $CaSiO_3$, with its peculiar silicate chain repeat length of three tetrahedral units (Deer et al., 1966), relaxes in a glass to a chain structure more like that of the pyroxenes $CaMgSi_2O_6$ and $MgSiO_3$.

Silica glass

Before the effect of network-modifying cations on the structure of aluminum-bearing framework silicates is analyzed, an examination of SiO_2 glass itself is warranted. On the basis of RDF analysis (Konnert and Karle, 1973) and Raman spectroscopy (Seifert et al., 1982), silica glass is believed to consist for the most part of interconnected six-membered rings of silicate tetrahedra, similar to a distorted tridymite. Additionally, there is Raman evidence for four-membered rings (Sharma et al., 1981). Although every silicon is expected to be in a Q^4 tetrahedron, the distribution of Si–O–Si bond angles in this structure can give rise to a broadening of the MAS linewidth.

Our sample was a crushed piece of fused quartz glass tubing with a small amount of crystalline Mg_2SiO_4 added

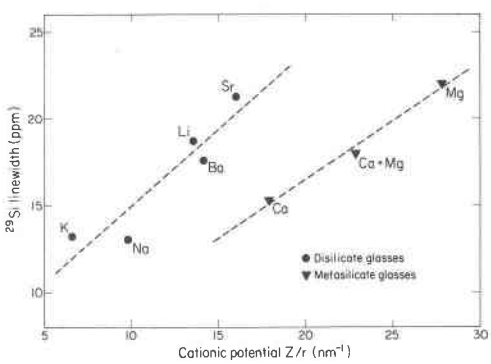

Fig. 5. Integrated linewidths (peak area/height) of disilicate and metasilicate glasses as a function of the ionic potential (charge/radius) of the network-modifying cation. Ionic radii are those of Shannon and Prewitt (1969). For $CaMgSi_2O_6$, the cationic potential was assumed to be the average of the values for Ca and Mg.

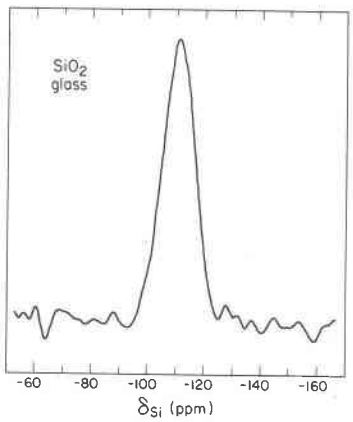

Fig. 6. ^{29}Si MAS NMR spectrum of silica glass, obtained by averaging 433 free-induction decays.

as an internal shift reference; its ^{29}Si MAS spectrum appears in Figure 6. The signal-to-noise ratio is relatively poor because a long silicon spin-lattice (T_1) relaxation time limited the rate at which successive free induction decays could be collected. (Radiofrequency pulses with a flip angle of $\sim 15°$ were spaced at 6 minute intervals). SiO_2 glass containing a small amount of dissolved paramagnetic Fe_2O_3 ($\sim 0.1\%$) would have a shorter relaxation time (Mosel et al., 1974), but we were unable to prepare such a sample with available apparatus.

In Figure 6, the SiO_2 peak maximum lies at -110.9 ppm, and the full width at half maximum (FWHM) is 13.2 ppm, from -103.8 to -117.0 ppm. These chemical shifts can be converted to a range of average Si–O–Si bond angles using the empirical formulas of Smith and Blackwell (1983) or Thomas et al. (1983a). One obtains a corresponding range of angles from roughly 135° to 160°, a result in qualitative agreement with the molecular dynamics (MD) calculations of Mitra (1982) and of Gaskell and Tarrant (1980). (It should be noted, however, that these authors present distributions for individual Si–O–Si angles, whereas the NMR linewidth reflects a range of values for the average over four Si–O–Si angles). The angle corresponding to the NMR peak maximum is 148°, which compares well with the average Si–O–Si angle derived from RDF work (150°) (Konnert and Karle, 1973), as well as MD values [e.g., 153° (Mitra, 1982)].

Dupree and Pettifer (1984) have recently presented a more detailed anlysis of the Si–O–Si bond angle distribution associated with a ^{29}Si MAS NMR spectrum of vitreous silica, but their peak maximum appears to lie at -109 ppm, corresponding to an average angle of 145.5°.

Aluminosilicate glasses

Our focus now turns to aluminum-bearing glasses, specifically tectosilicate glasses in which aluminum is believed to act as a network-forming cation, substituting for Q^4 silicons in tetrahedral units rather than changing the degree of polymerization in the role of an octahedrally coordinated network modifier (see Mysen et al., 1982, or Sharma et al., 1983). The type of equilibrium that can be affected by the identity of an alkali or alkaline earth cation now involves silicon-aluminum distributions instead of variations in Q^n populations. If we let Q^4(kAl) stand for a 3-D framework silicate tetrahedron linked via oxygen to k aluminate tetrahedra ($0 < k < 4$), we can imagine the following type of equilibrium condition (McMillan et al., 1982):

$$2Q^4(kAl) \rightleftharpoons Q^4[(k+1)Al] + Q^4[(k-1)Al]. \quad (5)$$

By analogy to the results obtained for metasilicate and disilicate glasses, we expect strongly polarizing cations to shift this equilibrium to the right, clustering cations near the aluminate tetrahedra linked to the $Q^4[(k+1)Al]$ silicate species and giving rise to more variety in the number of aluminate neighbors around different silicons. Raman spectra reported by McMillan et al. (1982) support this mechanism.

This trend is indeed apparent in Figure 7, which displays the ^{29}Si MAS spectra of glasses with a 3:1 Si/Al ratio: $KAlSi_3O_8$ (K-feldspar), $NaAlSi_3O_8$ (albite), and $Ca_{0.5}AlSi_3O_8$. (This latter composition is equivalent to $CaAl_2Si_2O_8 \cdot 4SiO_2$ and thus will be referred to as anorthite–4-quartz or An4Q.) Peak positions and integrated linewidths are given in Table 4 along with the chemical shifts of the corresponding crystalline alkali feldspars. [These contain only Q^4(1Al) and Q^4(2Al) silicons (Smith, 1974).] The glass peaks grow broader as the cation polarizing power increases from K^+ to Na^+ to Ca^{2+}, reflecting a widening distribution of Q^4(kAl) species and probably a widening distribution of Q^4 Si–O–T angles as well (T = Si,Al). As evidence for this latter statement, we note that RDF measurements on $NaAlSi_3O_8$ and $KAlSi_3O_8$ glasses suggest the presence of six-membered tridymite rings stuffed with alkali cations (Taylor and Brown, 1979a),

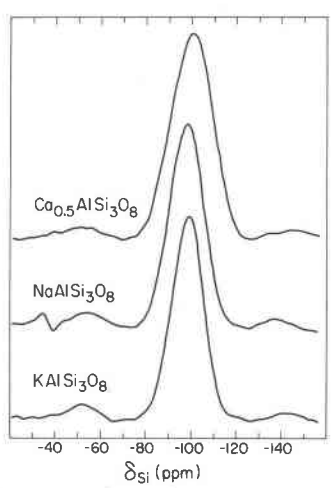

Fig. 7. ^{29}Si MAS NMR spectra of tectosilicate glasses with Si/Al = 3. The wiggle to the left of the albite spectrum is an artifact.

Table 4. Isotropic peak positions and linewidths in the ^{29}Si MAS NMR spectra of crystalline and glassy tectosilicates

Formula	Si/Al	Crystalline chemical shift (s) (ppm)	Peak position in glass (ppm)	Integrated linewidth of glass peak (ppm)
$KAlSi_3O_8$	3	-95.0,-98.0,-101.0	-99.0	17.3
$NaAlSi_3O_8$	3	-93.0,-97.0,-105.0	-97.9	18.0
$NaAlSi_2O_6$	2	-	-92.8	18.3
$NaAlSiO_4$*	1	85.0**	-86.0	13.3
$CaAl_2Si_{12}O_{28}$	6	-	-107.1	19.3
$CaAl_2Si_6O_{16}$	3	-	-101.0	22.3
$CaAl_2Si_4O_{12}$	2	-	-95.6	21.3
$CaAl_2Si_2O_8$	1	-82.5,-84.5,-89.5†	-86.5	17.1
$CaAl_2SiO_6$	0.5	-	-82.3	13.9
SiO_2	∞	-108.5††	-110.9	13.6

*Electron microprobe analysis of the natural crystalline sample yielded the approximate formula $Na_{3.03}K_{0.70}Si_{4.22}Al_{3.78}(Fe_{0.02}Ca_{0.01})O_{16}$ (Si/Al=1.12). The glass was prepared synthetically as $NaAlSiO_4$.

**Additional small peaks occur at -88.5 and -92.5 ppm which we assign to Q^4(3Al) and Q^4(2Al) silicons respectively. These appear because Si/Al > 1.

†Multiple peaks reflect crystallographically distinct Q^4(4Al) silicon sites.

††Cristobalite, Smith and Blackwell, 1983.

whereas the Raman spectrum of An4Q glass has been interpreted in terms of both six-membered SiO_2 rings and four-membered $Al_2Si_2O_8^{2-}$ rings (Seifert et al., 1982). The existence of two ring sizes would be expected to result in a wider range of inter-tetrahedral angles.

Figure 8 compares the ^{29}Si spectra of two tectoaluminosilicate glasses with a Si/Al ratio of unity: $NaAlSiO_4$ (nepheline) and $CaAl_2Si_2O_8$ (anorthite). In the corresponding crystals (see Table 4), silicon and aluminum cations are generally assumed to strictly alternate in the tetrahedral framework—each silicon is surrounded by four aluminums and *vice-versa*. [However, Sharma et al. (1983) have recently detected weak bands in the Raman spectrum of crystalline $CaAl_2Si_2O_8$ that imply some imperfection in the ordering.] The alternating arrangement of Al and Si is a manifestation of Loewenstein's aluminum-avoidance rule (Loewenstein, 1954), which states that Al–O–Al linkages between aluminate tetrahedra are energetically unfavorable. If this principle holds in glasses as well, then equilibria such as (5) are not important since every silicate tetrahedron must be a Q^4(4Al) unit.

Integrated linewidths for both sets of glasses are plotted as a function of cation polarizing power in Figure 9. Inspection of Figure 8 or Figure 9 reveals that the width of the anorthite glass peak exceeds that of nepheline glass. One cause for this difference might again be a greater range of bond angles in the anorthite glass. RDF measurements

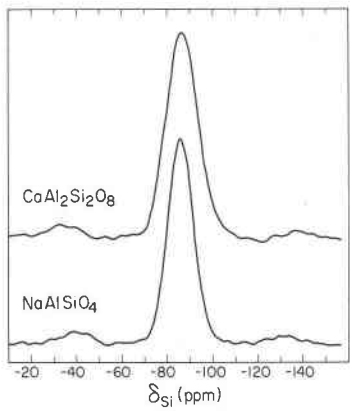

Fig. 8. ^{29}Si MAS NMR spectra of tectosilicate glasses with Si/Al = 1.

(Taylor and Brown, 1979a, 1979b) have indicated that the two glasses have markedly different structures: six-membered, "stuffed tridymite" rings in nepheline glass, four-membered feldspar-like rings in anorthite glass. The smaller rings may well entail more variety in bond angles. What is more, on the basis of Raman data, Seifert et al. (1982) have postulated the existence of a small quantity of six-membered rings in addition to the four-membered rings in $CaAl_2Si_2O_8$ glass. This variation in structure would be expected to create a wider range of bond angles.

Another possibility is that the greater polarizing power of calcium inspires a breakdown in aluminum avoidance. Indeed, Sharma et al. (1983) have seen evidence in their Raman spectra of Si–Al disorder in anorthite glass. That the increase in width of the anorthite peak versus the nepheline peak in Figure 8 is mainly an expansion into more negative chemical shifts is also an indication that Q^4(3Al) silicate tetrahedra may well be present in anorthite glass.

It should be noted, however, than when examined as a function of the Si/Al ratio, the linewidths of Figure 7 and 8

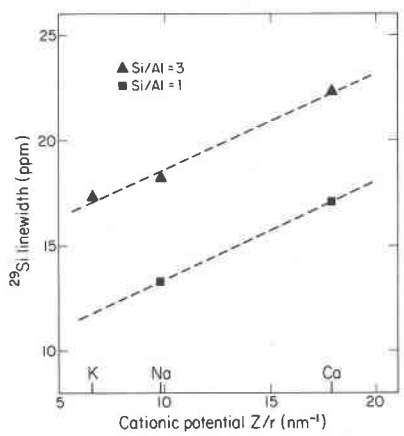

Fig. 9. Integrated linewidths of tectosilicate glasses as a function of cationic potential for different silicon-to-aluminum ratios. Linewidths increase with increasing cation polarizing power.

are consistent with substantial adherence to Loewenstein's rule. Specifically, the width of the albite glass peak is 4.9 ppm greater than that of nepheline glass, and the width of the An4Q glass peak is 5.2 ppm greater than that of anorthite glass. In short, glasses for which substantial rearrangement of Si and Al cations is possible without creating Al–O–Al linkages have broader linewidths than those for which compliance with the aluminum-avoidance principle imposes a rigid ordering scheme.

This argument can be generalized somewhat by considering a statistical model for silicon-aluminum ordering, with and without the aluminum-avoidance constraint. Let R be the Si/Al ratio in a 3-D framework glass. Without the restrictions of aluminum avoidance, the relative occurrence of a $Q^4(kAl)$ silicate tetrahedron is given simply by the probability of choosing k aluminum neighbors and $(4 - k)$ silicon neighbors:

$$P(k) = \binom{4}{k} \frac{R^{(4-k)}}{(R+1)^4}, \tag{6}$$

where the binomial coefficient is defined as

$$\binom{4}{k} = \frac{4!}{k!(4-k)!}. \tag{7}$$

With this probability distribution, the average number of aluminum neighbors (which governs the location of the ^{29}Si peak maximum) is given by

$$\langle k \rangle = \frac{4}{(R+1)}. \tag{8}$$

(Strictly speaking, the peak maximum will correspond to the average value of k only for a symmetric lineshape, but the difference between $\langle k \rangle$ and its most probable value is not important.) The variance in the number of aluminum neighbors (which contributes to the NMR lindwidth) is given by

$$\sigma^2 = \langle k^2 \rangle - \langle k \rangle^2 = \frac{4R}{(R+1)^2}. \tag{9}$$

The variance is a maximum ($\sigma^2 = 1$) when $R = 1$; i.e., for a composition like that of anorthite or nepheline. For $R = 3$ as in albite glass, $\sigma^2 = 0.75$.

In contrast, the imposition of aluminum avoidance requires four Si–O–Al linkages for each aluminum atom present. The relative occurrence of each $Q^4(kAl)$ silicate tetrahedron is given by

$$P(k) = \binom{4}{k} \frac{(R-1)^{(4-k)}}{R^4} \tag{10}$$

(Klinowski et al., 1982). Now $\langle k \rangle = 4/R$ and

$$\sigma^2 = \langle k^2 \rangle - \langle k \rangle^2 = \frac{4(R-1)}{R^2}. \tag{11}$$

In this case the variance is zero (no disorder) for $R = 1$, achieves its maximum value of 1.00 for $R = 2$, and falls to 0.89 for $R = 3$.

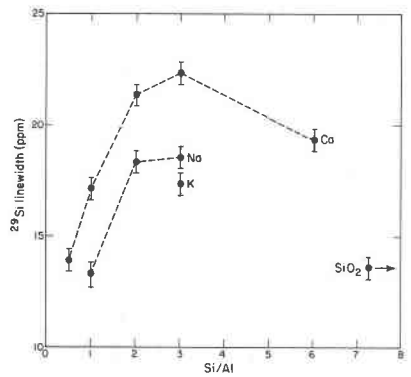

Fig. 10. Integrated linewidths of tectosilicate glasses as a function of R = Si/Al for different charge-balancing cations.

As noted above, the variance of k contributes at least in part to the NMR linewidth of aluminosilicate glasses. To explore this effect, we have collected ^{29}Si spectra for jadeite ($NaAlSi_2O_6$) glass and a series of glasses of the formula $CaAl_2O_4 \cdot nSiO_2$ (n = 1, 2, 4, 6, 12). Results are included in Table 4 and Figure 10, and are clearly more consistent with an aluminum avoidance effect than with its absence. However, linewidth maxima for both Na and Ca glasses occur near to R = 3, not R = 2. This perhaps indicates that other contributions to linewidth, such as variance in Si–O–T bond angles, also increase with the Si/Al ratio. Such a conclusion is supported by the molecular orbital calculations of Geisinger et al. (1984), which suggest that as the Si–O–T angle varies from its most stable value, energies increase more rapidly for Si–O–Al than for Si–O–Si.

In comparison, a ^{29}Si MAS NMR study of three gallosilicate glasses (G. S. Henderson and J. B. Murdoch, unpublished data) has shown that isotropic linewidths increase in accord with a statistical model of "gallium avoidance":

$$NaGaSiO_4 < NaGaSi_3O_8 \lesssim NaGaSi_2O_6. \tag{12}$$

[Like aluminum, gallium has a deshielding effect on neighboring ^{29}Si nuclei (Vaughan et al., 1983).]

Natural composition glasses

To investigate the usefulness of ^{29}Si MAS NMR in the analysis of magmas, we turn finally to three glasses made experimentally from Fe-poor silicic lavas collected at Mono Craters (A), Mt. Lassen (B), and Mt. Shasta (C). All three were remelted under reducing conditions in graphite crucibles; calculations using the results of Kilinc et al. (1983) indicate that >99% of the iron present is Fe^{2+}. Table 5 gives the chemical analysis and CIPW norm of each, plus the Si/Al ratio and the number of non-bridging oxygens per tetrahedral cation (NBO/T). Rhyolitic glass A can be represented an approximately one third silica glass, one third albite glass, and one third K-feldspar glass. In going to glasses B and C, the K-feldspar component is partially replaced by anorthite and the number of non-bridging oxygens increases, indicating a drop in the

average degree of polymerization. Nevertheless, all three glasses are expected to have predominantly three-dimensional framework structures, i.e., a predominance of Q^4 tetrahedra.

The ^{29}Si NMR spectra of the natural composition glasses are displayed in Figure 11. The first trend to strike the eye is the increase in spinning sideband intensity in going from A to B to C. This change is not related to a massive increase in chemical shielding anisotropy but rather to an increase in concentration of paramagnetic Fe^{2+} ions. Magnetic dipole–dipole coupling between the rapidly relaxing unpaired electrons on the iron and nearby silicon-29 nuclei induces a paramagnetic shift in the NMR spectra of these nuclei. The form of this largely inhomogeneous shift is similar to that of a chemical shift, but the magnitude can be much greater (Sanz and Stone, 1977). As the concentration of iron increases, the number of silicon nuclei affected by paramagnetic shifts in turn rises; as a result, spinning sidebands cover a wider range of frequencies and become more intense. Oldfield et al. (1983) have reported a similar effect in minerals caused by ferromagnetic inclusions, but such inclusions were not observed microscopically in these glasses.

The overall spectral intensity (including sidebands) also drops in going from A to B to C; the relative values are 1.00:0.70:0.37. This drop too is a function of increasing paramagnetic content. Those silicon nuclei that are located very near unpaired electrons not only experience a large shift but also relax rapidly (Abragam, 1961, Chap. 9). Both effects can cause such severe broadening that these perturbed silicons are not seen at all in the spectrum.

The linewidths and chemical shifts of the three center peaks are collected in Table 6. An unambiguous analysis is difficult because in going from A to B to C, two factors—the decrease in the Si/Al ratio R *and* the increase in the number of non-bridging oxygens—would be expected to broaden the peak and shift its maximum to less negative values of δ. Moreover, additional broadening is caused by the paramagnetic ions present, as found by Grimmer et al. (1983a) in a study of Fe,Mg substitution in synthetic olivines.

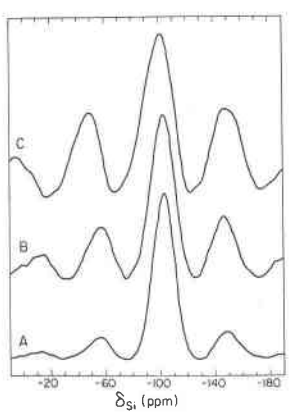

Fig. 11. ^{29}Si MAS NMR spectra of glasses made from lava collected at Mono Craters (A), Mt. Lassen (B), and Mt. Shasta (C), California. All three are drawn to the same height, but the number of observable silicons and hence the measured signal intensity decrease in going from A to B to C.

Table 5. Analysis of natural composition glasses

		Glass A	Glass B	Glass C
Chemical constituents* (wt %)				
	SiO_2	74.98	69.16	61.17
	TiO_2	0.07	0.38	0.69
	Al_2O_3	12.30	14.81	16.58
	FeO	1.01	2.42	4.41
	MnO	0.05	0.06	0.08
	MgO	0.04	1.41	4.03
	CaO	0.60	3.00	6.73
	Na_2O	4.01	4.30	4.21
	K_2O	4.66	2.73	1.05
CIPW norm (wt %)				
	SiO_2	31.90	23.78	11.19
	$KAlSi_3O_8$	27.54	16.13	6.20
	$NaAlSi_3O_8$	33.93	36.39	35.62
	$CaAl_2Si_2O_8$	1.80	13.05	23.24
	$Ca(Mg,Fe)Si_2O_6$	1.04	1.53	8.30
	$(Mg,Fe)SiO_3$	1.38	6.68	13.08
	$FeTiO_3$	0.13	0.72	1.31
NBO/T**		0.027	0.105	0.294
Si/Al ratio		5.17	3.96	3.13

*P_2O_5 ignored and all iron assumed to be Fe^{2+}
**calculated according to Mysen et al. (1982)

The location of the peak maximum, however, is largely dependent on the Si/Al ratio. From Table 4, the average chemical shift for alkali feldspar glasses is roughly −98.5 ppm; the average number of aluminum neighbors per silicate tetrahedron is 4/3 = 1.33. In comparison, the silica glass NMR peak lies at −111 ppm and $\langle k \rangle = 0$. From these two data pairs, we get the following simple relationship:

$$\delta \text{ (ppm)} = -111 + 9.4 \langle k \rangle$$
$$= -111 + 37.5/R. \quad (13)$$

Using values for R in Table 5, one can predict that the peak maxima should lie at −103.5, −101.5, and −99.0 ppm for samples A, B, and C. These numbers are indeed close to the experimental results in Table 6.

Conclusions

For the disilicate and metasilicate glasses investigated here, ^{29}Si MAS NMR spectra indicate that the predominant Q^n silicate unit in the glass is the one found in the

Table 6. Isotropic peak positions and linewidths in the ^{29}Si MAS NMR spectra of natural composition glasses

Glass	Peak position (ppm from TMS)	FWHM (ppm)
A	-103.5	19.0
B	-101.8	21.7
C	-99.8	24.8

corresponding crystalline material, and that the range of silicate species present increases with smaller, more highly charged network-modifying cations. Similarly, such cations probably induce greater variety in the distribution of Si and Al in tectosilicate glasses. The dependence of linewidth on the Si/Al ratio indicates, however, than an aluminum avoidance effect is present. In silica glass itself, the MAS linewidth reflects a range of average bond angles from $\sim 135°$ to $\sim 160°$, a result in good agreement with RDF and MD findings.

Because our one measurable parameter, the isotropic chemical shift, is sensitive to a variety of structural features affecting a silicon-29 nucleus—the number of non-bridging oxygens, the identity of neighboring tetrahedral cations, bond angle values, and the presence of nearby paramagnetic ions—the spectra of multicomponent glasses cannot be readily interpreted. Nonetheless, the location of peak maxima for the three natural composition glasses we examined can be correlated with the Si/Al ratio.

Note added in proof:

Recently, Schramm et al. (1984) have published spectra for a series of lithium silicate glasses and crystals, and have deconvoluted glass spectra to estimate distributions of Q^n species, a range of which was apparent in all compositions. Their reported fractions of Q^2 and Q^4 in $Li_2Si_2O_5$ glass are somewhat higher than those given here. They show partially resolved double peaks in high silica glasses, as we saw in $Na_2Si_4O_9$ glass, but many of their samples were apparently phase separated. Grimmer et al. (1984) have reported spectra on both sodium and lithium silicate glasses which are generally similar to ours and those of Schramm et al. (1984). These authors have chosen a markedly different interpretation, however, by assuming that single Q^n species are present unless separate peaks are clearly resolved. We feel the widths of observed NMR peaks, the results of Raman spectroscopy mentioned above, and thermodynamic considerations, all make a distribution of species more likely to be correct.

Acknowledgments

We are grateful to Professor A. Pines (Univeristy of California) for the use of his NMR facilities as well as his continuing interest in this and related work on aluminosilicate structure. We would also like to thank Dr. S. K. Sharma for providing copies of his Raman work prior to publication, M. L. Rivers and R. Lange for preparing several of the glasses, and D. F. Weill (University of Oregon) for supplying the $KAlSi_3O_8$ and An4Q glass samples.

This work was supported by the Director, Office of Basic Energy Sciences, Division of Engineering, Mathematics, and Geosciences, of the U.S. Department of Energy under contract DE-AC03-76SF00098.

References

Abragam, A. (1961) The Principles of Nuclear Magnetism. Oxford University Press, London.

Andrew, E. R. (1972) The narrowing of NMR spectra of solids by high-speed specimen rotation and the resolution of chemical shift and spin multiplet structures for solids. Progress in NMR spectroscopy, 8, 1–39.

Brawer, S. A. and White, W. B. (1975) Raman spectroscopic investigation of the structure of silicate glasses. I. The binary alkali silicates. Journal of Chemical Physics, 63, 2421–2432.

Charles, R. J. (1967) Activities in the Li_2O–Na_2O and K_2O–SiO_2 solutions. Journal of the American Ceramic Society, 50, 631–640.

Deer, W. A., Howie, R. A., and Zussman, J. (1977) An Introduction to Rock-Forming Minerals. Longman, London.

de Jong, B. H. W. S. and Schramm, C. M. (1981) Comparison of silica species distribution in vitreous and partially devitrified $Li_2O \cdot 2SiO_2$ glass by magic angle spinning ^{29}Si NMR. (abstr.) Transactions of the American Geophysical Union (EOS), 45, 1070.

de Jong, B. H. W. S., Schramm, C. M., and Parziale, V. E. (1983) Polymerization of silicate and aluminate tetrahedra in glasses, melts, and aqueous solutions—IV. Aluminum coordination in glasses and aqueous solutions and comments on the aluminum avoidance principle. Geochimica et Cosmochimica Acta, 47, 1223–1236.

de Jong, B. H. W. S., Keefer, K. D., Brown, G. E., and Taylor, C. M. (1981) Polymerization of silicate and aluminate tetrahedra in glasses, melts, and aqueous solutions—III. Local silicon environments and internal nucleation in silicate glasses. Geochimica et Cosmochimica Acta, 45, 1291–1308.

Dupree, E. and Pettifer, R. F. (1984) Determination of the Si–O–Si bond angle distribution in vitreous silica by magic angle spinning NMR. Nature, 308, 523–525.

Engelhardt, G., Zeigan, D., Jancke, H., Hoebbel, D. and Weiker, W. (1975) Zur Abhängigkeit der Struktur der Silicatanionen in wassrigen Natriumsilicatlosugen vom Na : Si verhältnis. Zeitschrift für Anorganische und Allgemeine Chemie, 418, 17–28.

Gaskell, P. H. and Tarrant, I. D. (1980) Refinement of a random network model for vitreous silicon dioxide. Philosophical Magazine, B42, 265–286.

Geisinger, K. L., Gibbs, G. V., and Navrotsky, A. (1984) A molecular orbital study of bond length and angle variations in framework silicates. Journal of Non-Crystalline Solids, 68, 401–402.

Grimmer, A.-R., von Lampe, F., Mägi, M., and Lippmaa, E. (1983a) Hochauflösende ^{29}Si-NMR an festen Silicaten; Einfluss von Fe^{2+} in Olivinen. Zeitschrift für Chemie, 23, 343–344.

Grimmer, A.-R., von Lampe, F., Mägi, M., and Lippmaa, E. (1983b) Hochauflösende ^{29}Si-Festkörper–NMR–Spektroskopie: Si–O–Si-Bindungswinkel und chemische Verschiebung in Disilicaten. Monatshefte für Chemie, 114, 1053–1057.

Grimmer, A.-R., von Lampe, F., Tarmak, M., and Lippmaa, E. (1983c) Solid-state high-resolution ^{29}Si NMR in zunyite. Chemical Physics Letters, 97, 185–187.

Grimmer, A.-R., Mägi, M., Hähnert, M., Stade, H., Samoson, A.,

Weiker, W., and Lippmaa, E. (1984) High-resolution solid-state ^{29}Si nuclear magnetic resonance studies of binary alkali silicate glasses. Physics and Chemistry of Glasses, 25, 105–109.

Harris, I. A. and Bray, P. J. (1980) ^{29}Si NMR spectra of glasses and polycrystalline compounds in the system K_2O–SiO_2. Physics and Chemistry of Glasses, 21, 156–159.

Herzfeld, J. and Berger, A. E. (1980) Sideband intensities in NMR spectra of samples spinning at the magic angle. Journal of Chemical Physics, 73, 6021–6030.

Higgins, J. B. and Woessner, D. E. (1982) ^{29}Si, ^{27}Al, and ^{23}Na spectra of framework silicates. (abstr.) Transactions of the American Geophysical Union (EOS), 63, 1139.

Holzman, G. R., Lauterbur, P. C., Anderson, J. H., and Koth, W. (1956) Nuclear magnetic resonance field shifts of ^{29}Si in various materials. Journal of Chemical Physics, 25, 172–173.

Imaoka, M., Hasegawa, H., and Yasui, I. (1983) X-ray diffraction study of the structure of silicate glasses. Part 2. Alkali disilicate glasses. Physics and Chemistry of Glasses, 24, 72–78.

Kilinc, A. I., Carmichael, I. S. E., Rivers, M. L., and Sack, R. O. (1983) The ferric-ferrous ratio of natural silicate liquids equilibrated in air. Contributions to Mineralogy and Petrology, 83, 136–140.

Kirkpatrick, R. J., Smith, K. A., Kinsey, R. A., and Oldfield, E. (1982) High-resolution ^{29}Si NMR of glasses and crystals in the system CaO–MgO–SiO_2. (abstr.) Transactions of the American Geophysical Union (EOS), 63, 1140.

Klinowski, J., Ramdas, S., Thomas, J. M., Fyfe, C. A., and Hartman, J. S. (1982) A re-examination of Si,Al ordering in zeolites NaX and NaY. Journal of the Chemical Society, Faraday Transactions II, 78, 1025–1050.

Konnert, J. H. and Karle, J. (1973) The computation of radial distribution functions for glassy materials. Acta Crystallographica, A29, 702–710.

Lippmaa, E., Mägi, M., Samoson, A., Engelhardt, G., and Grimmer, A.-R. (1980) Structural studies of silicates by solid-state high-resolution ^{29}Si NMR. Journal of the American Chemical Society, 102, 4889–4893.

Lippmaa, E., Magi, M., Samoson, A., Tarmak, M., and Engelhardt, G. (1981) Investigation of the structure of zeolites by solid-state high-resolution ^{29}Si NMR spectroscopy. Journal of the American Chemical Society, 103, 4992–4996.

Lippmaa, E., Samoson, A., Mägi, M., Teeäär, R., Schraml, J., and Götz, J. (1982) High resolution ^{29}Si NMR study of the structure and devitrification of lead-silicate glasses. Journal of Non-Crystalline Solids, 50, 215–218.

Loewenstein, W. (1954) The distribution of aluminum in the tetrahedra of silicates and aluminates. American Mineralogist, 39, 92–96.

Mägi, M., Lippmaa, E., Samoson, A., Engelhardt, G., and Grimmer, A. R. (1984) Solid-state high-resolution silicon-29 chemical shifts in silicates. Journal of Physical Chemistry, 88, 1518–1522.

Maricq, M. M. and Waugh, J. S. (1979) NMR in rotating solids. Journal of Chemical Physics, 70, 3300–3316.

Matson, D. W., Sharma, S. K., and Philpotts, J. A. (1983) The structure of high-silica alkali-silicate glasses. A Raman spectroscopic investigation. Journal of Non-Crystalline Solids, 58, 323–352.

McMillan, P., Piriou, B., and Navrotsky, A. (1982) A Raman spectroscopic study of glasses along the joins silica-calcium aluminate, silica-sodium aluminate, and silica-potassium aluminate. Geochimica et Cosmochimica Acta, 46, 2021–2037.

McMillan, P. (1984a) Structural studies of silicate glasses and melts—applications and limitations of Raman spectroscopy. American Mineralogist, 69, 622–644.

McMillan, P. (1984b) A Raman spectroscopic study of glasses in the system CaO–MgO–SiO_2. American Mineralogist, 69, 645–659.

Mysen, B. O., Virgo, D., and Seifert, F. A. (1982) The structure of silicate melts: implications for the chemical and physical properties of natural magmas. Reviews of Geophysics and Space Physics, 20, 353–383.

Ohashi, Y. and Finger, L. W. (1976) The effect of Ca substitution on the structure of clinoenstatite. Carnegie Institution of Washington Year Book, 75, 743–746.

Oldfield, E., Kinsey, R. A., Smith, K. A., Nichols, J. A., and Kirkpatrick, R. J. (1983) High-resolution NMR of inorganic solids. Influence of magnetic centers on magic-angle sample-spinning lineshapes in some natural aluminosilicates. Journal of Magnetic Resonance, 51, 325–329.

Ramdas, S. and Klinowski, J. (1984) A simple correlation between isotropic ^{29}Si-NMR chemical shifts and T–O–T angles in zeolite frameworks. Nature, 308, 521–523.

Sanz, J. and Stone, W. E. E. (1977) NMR study of micas. I. Distribution of Fe^{2+} ions on the octahedral sites. Journal of Chemical Physics, 67, 3739–3743.

Schramm, C. M., DeJong, B. H. W. S., and Parziale, V. E. (1984) ^{29}Si Magic angle spinning NMR study on local silicon environments in amorphous and crystalline lithium silicates.

Seifert, F., Mysen, B. O., and Virgo, D. (1982) Three-dimensional network structure of quenched melts (glass) in the systems SiO_2–$NaAlO_2$, SiO_2–$CaAl_2O_4$ and SiO_2–$MgAl_2O_4$. American Mineralogist, 67, 696–717.

Shannon, R. D. and Prewitt, C. T. (1969) Effective ionic radii in oxides and fluorides. Acta Crystallographica, B25, 925–946.

Sharma, S. K., Mammone, J. F. and Nicol, M. F. (1981) Raman investigation of ring configurations in vitreous silica. Nature, 292, 140–141.

Sharma, S. K., Simons, B., and Yoder, H. S. (1983) Raman study of anorthite, calcium Tschermak's pyroxene, and gehlenite in crystalline and glassy states. American Mineralogist, 68, 1113–1125.

Smith, J. V. (1974) Feldspar Minerals, Vol. I, Crystal Structure and Physical Properties. Springer-Verlag. Berlin.

Smith, J. V. and Blackwell, C. S. (1983) Nuclear magnetic resonance of silica polymorphs. Nature, 303, 223–225.

Smith, K. A., Kirkpatrick, R. J., Oldfield, E., and Henderson, D. M. (1983) High-resolution silicon-29 nuclear magnetic resonance spectroscopic study of rock-forming silicates. American Mineralogist, 68, 1206–1215.

Taylor, M. and Brown, G. E. (1979a) Structure of mineral glasses—I. The feldspar glasses $NaAlSi_3O_8$, $KAlSi_3O_8$, and $CaAl_2Si_2O_8$. Geochimica et Cosmochimica Acta, 43, 61–75.

Taylor, M. and Brown, G. E. (1979b) Structure of mineral glasses—II. The SiO_2–$NaAlSiO_4$ join. Geochimica et Cosmochimica Acta, 43, 1467–1473.

Thomas, J. M., Klinowski, J., Ramdas, S., Hunter, B. K., and Tennakoon, D. T. B. (1983a) The evaluation of non-equivalent tetrahedral sites from ^{29}Si NMR chemical shifts in zeolites and related aluminosilicates. Chemical Physics Letters, 102, 158–162.

Thomas, J. M., Klinowski, J., Ramdas, S., Anderson, M. W., Fyfe, C. A., and Gobbi, G. C. (1983b) New approaches to the structural characterization of zeolites: Magic-angle spinning NMR (MASNMR). In G. D. Stucky and F. G. Dwyer, Eds., Intrazeol-

ite Chemistry, p. 159–180. American Chemical Society, Washington, D. C.

Tomozawa, M. (1972) Liquid phase separation and crystal nucleation in Li_2O–SiO_2 glasses. Physics and Chemistry of Glasses, 13, 161–166.

Vaughan, D. E. W., Melchior, M. T., and Jacobson, A. J. (1983) High resolution silicon-29 NMR studies of gallium faujasites and a gallium sodalite. In G. D. Stucky and F. G. Dwyer, Eds., Intrazeolite Chemistry, p. 231–242. American Chemical Society, Washington, D. C.

Virgo, D., Mysen, B. O., and Kushiro, I. (1980) Anionic constitution of 1-atmosphere silicate melts: Implications for the structure of igneous melts. Science, 208, 1371–1373.

Manuscript received, March 15, 1984;
accepted for publication, November 19, 1984.